Available online at www.sciencedirect.com
ScienceDirect
Biochimica et Biophysica Acta 1778 (2008) 896–906
Biochimica et Biophysica Acta BBA
www.elsevier.com/locate/bbamem

Delivery of the Cu-transporting ATPase ATP7B to the plasma membrane in *Xenopus* oocytes

Éva Lörinczi [a,1], Ruslan Tsivkovskii [b], Winfried Haase [a], Ernst Bamberg [a], Svetlana Lutsenko [b,*], Thomas Friedrich [a,*,2]

[a] *From the Max-Planck-Institute of Biophysics, D-60438 Frankfurt am Main, Germany*
[b] *Oregon Health and Science University, Department of Biochemistry and Molecular Biology, 3181 SW Sam Jackson Park Road, Portland, OR 97239-3098, USA*

Received 4 July 2007; received in revised form 11 December 2007; accepted 27 December 2007
Available online 3 January 2008

Abstract

Cu-transporting ATPase ATP7B (Wilson disease protein) is essential for the maintenance of intracellular copper concentration. In hepatocytes, ATP7B is required for copper excretion, which is thought to occur via a transient delivery of the ATP7B- and copper-containing vesicles to the apical membrane. The currently available experimental systems do not allow analysis of ATP7B at the cell surface. Using epitope insertion, we identified an extracellular loop into which the HA-epitope can be introduced without inhibiting ATP7B activity. The HA-tagged ATP7B was expressed in *Xenopus* oocytes and the presence of ATP7B at the plasma membrane was demonstrated by electron microscopy, freeze-fracture experiments, and surface luminescence measurements in intact cells. Neither the deletion of the entire N-terminal copper-binding domain nor the inactivating mutation of catalytic Asp1027 affected delivery to the plasma membrane of oocytes. In contrast, surface targeting was decreased for the ATP7B variants with mutations in the ATP-binding site or the intra-membrane copper-binding site, suggesting that ligand-stabilized conformation(s) are important for ATP7B trafficking. The developed system provides significant advantages for studies that require access to both sides of ATP7B in the membrane.

Keywords: ATP7B; Copper; Wilson disease protein; Oocyte; Luminescence; Plasma membrane

1. Introduction

Copper is essential for cell metabolism and is required for organism growth and development. In humans, disruption of normal copper distribution results in severe metabolic disorders such as Wilson disease. Wilson disease [1] is associated with accumulation of copper in several tissues, the lack of copper incorporation into the secreted ferroxidase ceruloplasmin [2], and defective copper excretion from the liver into the bile. The syndrome is caused by mutations in the *ATP7B* gene, which encodes a copper-transporting ATPase ATP7B, also known as Wilson disease protein, WNDP [3,4]. ATP7B, together with a closely related Menkes disease protein (MNKP, ATP7A), belongs to a large family of membrane transporters called P-type ATPases [5], which utilize the energy of ATP hydrolysis to transport ions across cellular membranes.

Abbreviations: AP, alkaline phosphatase; ATP-BD, ATP-binding domain; ER, endoplasmic reticulum; HA, haemagglutinin A of influenza virus; HRP, horseradish peroxidase; MBS, metal-binding sites; MNKP, Menkes disease protein; NBD, nucleotide-binding domain; N-MBD, amino-terminal metal-binding domain; WNDP, Wilson disease protein; TGN, *trans*-Golgi network; TMS, transmembrane segment

* Corresponding authors. T. Friedrich is to be contacted at Technical University of Berlin, Institute of Chemistry, Secr. PC-14, Straße des 17. Juni 135, D-10623 Berlin, Germany. Tel.: +49 30 314 24128; fax: +49 30 314 21122. S. Lutsenko, tel.: +1 503 494 6953.
E-mail addresses: lutsenko@ohsu.edu (S. Lutsenko), friedrich@chem.tu-berlin.de (T. Friedrich).
[1] Present address: Max-Planck-Institute of Experimental Medicine, D-37075 Göttingen, Germany.
[2] Present address: Technical University of Berlin, Institute of Chemistry, D-10623 Berlin, Germany.

0005-2736/$ - see front matter © 2008 Elsevier B.V. All rights reserved.
doi:10.1016/j.bbamem.2007.12.020

In the liver, ATP7B has a dual role: under basal conditions it transports copper into the secretory pathway for biosynthesis of ceruloplasmin and, upon elevation of intracellular copper, it mediates removal of excess copper from the cell. This dual function is accomplished through the copper-dependent cycling of the protein between different cell compartments (Fig. 1A). It is generally accepted that in low copper, ATP7B is localized in the *trans*-Golgi network (TGN) of hepatocytes and that ATP7B leaves the TGN when copper is elevated [6,7]. The fate of ATP7B following its exit from TGN is less firmly established. The current data support two alternative models of ATP7B trafficking (Fig. 1A).

The consistently demonstrated redistribution of ATP7B to a vesicular compartment and the lack of substantial plasma membrane staining led to the proposal of a vesicle-mediated mechanism of copper clearance from the cells (Fig. 1A). In this model (pathway 1), ATP7B transports excess copper into vesicles, which then move to the plasma membrane and exocytose. ATP7B itself returns to the TGN without ever having reached the plasma membrane [8]. However, studies using polarized hepatocytes yielded data in favour of an alternative mechanism. Specifically, copper-dependent relocalisation of ATP7B to vesicular structures and to apical vacuoles reminiscent of bile canaliculi was demonstrated in cultured HepG2 cells [7]. This observation suggests that ATP7B in vesicles relocates to the apical membrane as a part of its recycling process and is retrieved back to the TGN when intracellular copper decreases (pathway 2). This second model is further supported by recent high-resolution microscopy studies from Guo et al., who demonstrated that in polarized WIF-cells, both endogenous and recombinant ATP7B can be detected at the plasma membrane by co-localization with the apical membrane marker anti-aminopeptidase N [9].

ATP7B is endogenously expressed in WIF and HepG2 cells, therefore these cells provide a relevant cellular environment for analysis of ATP7B trafficking. However, certain aspects of ATP7B structure, function, and regulation are very difficult to evaluate in these cells, because upon polarization their apical extracellular surface is not accessible for experimental manipulations. As a result, commonly used experimental procedures for analysis of plasma membrane delivery and retrieval, such as surface antibody binding or surface biotinylation, are extremely difficult to perform. Similarly, topological studies of ATP7B, analysis of conformational changes upon ligand binding, and interactions of ATP7B with proteins or other molecules at the extracellular (luminal) side cannot be carried out in either WIF or HepG2 cells. Yet, this information may provide important insights into regulation of ATP7B and the copper export mechanism. *Xenopus laevis* oocytes have been successfully employed for studies on biogenesis, assembly, and plasma membrane delivery of numerous transporters, including P-type ATPases [10–14]. Therefore, we utilized expression in *X. laevis* oocytes to develop a tractable system with access to both sides of ATP7B.

In addition to allowing quantitative measurements of plasma membrane delivery in living cells, the oocyte system can be very useful for the identification of structural elements required for ATP7B trafficking. Mammalian cells are extremely sensitive to changes in protein folding or protein flexibility. For example, when ATP7B bearing the His1069Gln mutation is expressed in mammalian cells at 37 °C, it is trapped in the endoplasmic reticulum (ER), indicating its inability to escape the ER quality control system [8]. However, the effect of this mutation on folding is very minor [15,16] and lowering the temperature

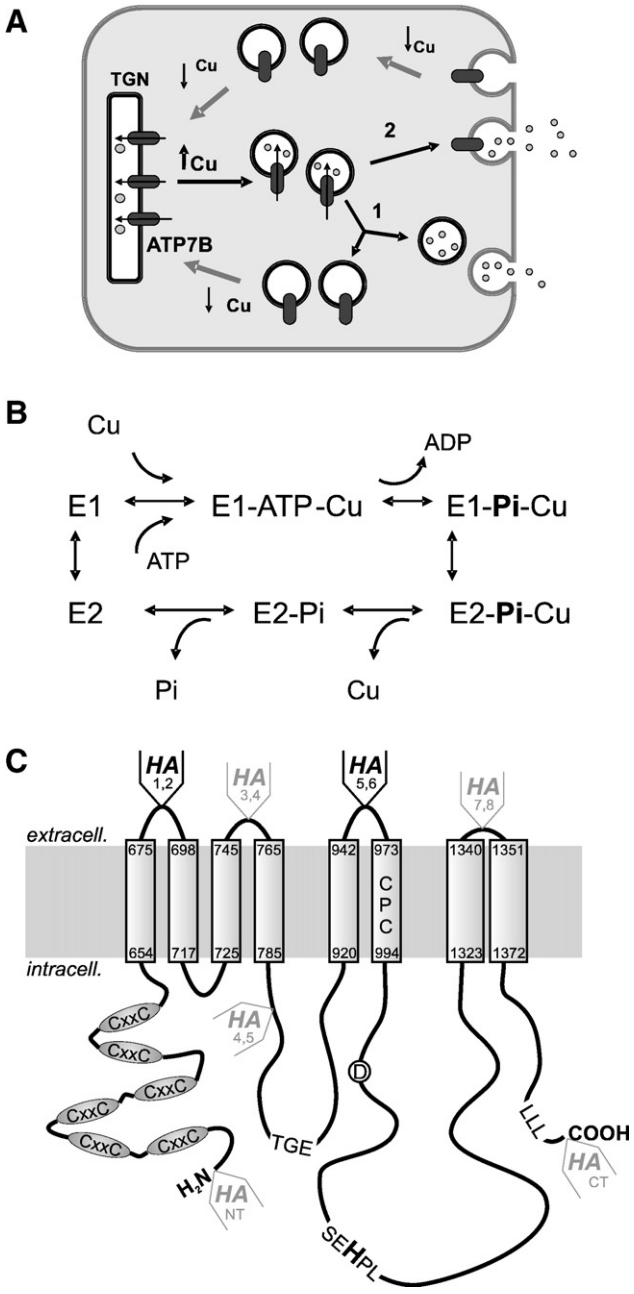

Fig. 1. (A) Two alternative models of ATP7B trafficking. Under regular (low copper) conditions ATP7B is primarily located in the *trans*-Golgi network (TGN). In elevated copper, ATP7B re-distributes to a vesicular compartment. Excess copper in vesicles is then removed via vesicle exocytosis, while ATP7B itself returns to TGN without reaching the plasma membrane [8]. Alternatively, ATP7B traffics with vesicles to the plasma membrane; the copper is then exported and ATP7B is retrieved back from the membrane to TGN. (B) The simplified catalytic cycle of ATP7B. (C) Transmembrane topology of ATP7B and the locations of the inserted HA-epitope tags. The amino-terminal domain with six copper-binding sites containing a CxxC motif, the highly conserved SEHPL motif including H1069, a site of common Wilson disease mutation, the intra-membrane copper-binding site CxC, and the triple leucine at the carboxy-terminus are shown. Encircled D denotes the phosphorylation site, Asp1027.

allows the protein to exit the ER and be targeted normally to the TGN [8]. This high sensitivity of mammalian cells to even minor changes in protein folding/stability complicates identification of structural elements required for trafficking *per se*. This is because partially mis-folded or simply flexible mutants may be retained in ER and not traffic even though the structural elements involved in interactions with the cell trafficking machinery are unaffected by the mutation. Oocytes require a lower temperature for their growth and are more permissive of slight changes in protein folding, perhaps due to slower protein dynamics [17]. This property of oocytes enabled us to characterize deletion mutants of ATP7B and narrow down the region required for the anterograde step of ATP7B trafficking.

Lastly, we sought to elucidate the relationship between enzymatic activity of ATP7B and its ability to leave the TGN. The catalytic cycle of ATP7B involves the binding of copper and ATP, followed by ATP hydrolysis via the formation of phosphorylated intermediate. Conformational changes then allow copper to be released at the opposite side of the membrane (Fig. 1B). Copper release stimulates protein dephosphorylation, completing the cycle. Previous studies from several laboratories provided convincing evidence that the inactivation of ATP7B may lead to the loss of the ability to traffic [18,19]. Furthermore, the triple mutation TGE>AAA (Fig. 1C), which blocks dephosphorylation, was shown to markedly diminish the TGN retention for both ATP7B and ATP7A [20]. This interesting finding led to the suggestion that the trafficking of copper-ATPases is initiated during the catalytic cycle each time the protein is phosphorylated by ATP [20]. However, more recent studies on various ATP7A mutants suggest that activity may not be obligatory for Cu-ATPase relocalisation [21]. We hypothesized that elevated copper stabilizes ATP7B in a certain conformation and that the ability of the protein to adopt this conformation, rather than activity itself is necessary for ATP7B trafficking. Our present data support this hypothesis.

2. Materials and methods

2.1. cDNA constructs

ATP7B cDNA was subcloned into the oocyte expression vector pTNPN (a derivative of pTLN [22] containing a PacI restriction site within the multiple cloning region). Specifically, a pMT2-ATP7B construct (originally from K. Petrukhin, Columbia University) was cut by SalI (completely) and EcoRI (partially) and the resulting 4.4 kb fragment was ligated into the EcoRI/XhoI-digested pTNPN, yielding the ATP7B-plasmid-1. To remove the non-coding 5′ region, PCR was performed using a forward adapter primer, which added a PacI site and a Kozak sequence for optimal eukaryotic translation initiation (GCCAC-C*ATG*G) immediately preceding the start-ATG, and a reverse primer, which bound downstream of the unique BspEI restriction site. The resulting PCR fragment was cut with PacI/BspEI and ligated into the appropriately cut ATP7B-plasmid-1, yielding the final ATP7B-pTNPN construct. The HA-epitope (YPYDVPDYA) and the extended HA-epitope (SEHYPYDVPDYAVTF) insertions (derived from the hemagglutinin A protein of human influenza virus), as well as deletions and mutations, were introduced by PCR at the following positions (Table 1): ATP7B-HA1,2 (after Val683), ATP7B-HA3,4 (after Ala756), ATP7B-HA4,5 (after Ser797), ATP7B-HA5,6 (after Asn-958), ATP7B-HA7,8 (after Ile1346), ATP7B-HA5,6-delN600 (deletion of Pro-2 to Ala600), and ATP7B-HA5,6-delLLL (truncation after Ser1453). The bacteriorhodopsin (BR) cDNA sequence was subcloned into pTLN vector, and the HA-epitope was introduced after the propeptide sequence at Ser13 in the BR sequence. All PCR-derived fragments were verified by sequencing (MWG Biotech AG, Ebersberg, Germany).

2.2. Oocyte preparation, cRNA synthesis and injection

Individual stage V to VI oocytes were isolated by collagenase treatment after surgical removal of ovarian lobes from anaesthetised *X. laevis* females. Synthesis of cRNA was carried out using the SP6 mMessage mMachine kit (Ambion, Huntingdon, U.K.) after linearization of DNA plasmid with MluI. 2.5 to 50 ng of ATP7B cRNA were injected into oocytes (50 nl injection volume). Following injection, oocytes were kept at 17 °C in MBS solution (in mM: 88 NaCl, 2.4 $NaHCO_3$, 1 KCl, 0.41 $CaCl_2$, 0.33 $Ca(NO_3)_2$, 0.82 $MgSO_4$, 10 Hepes, pH 7.6), or ORi solution (in mM: 115 NaCl, 5 KCl, 2 $CaCl_2$, 5 Hepes, pH 7.5).

2.3. Western blot analysis of protein expression

Crude membrane preparations were obtained by homogenizing oocytes in ice-cold lysis buffer (in mM: 250 sucrose, 0.5 EDTA, 5 Tris–HCl, pH 7.4) containing 1xComplete® and 4 mM Pefablock (Roche Molecular Biochemicals) and removal of yolk platelets by three low speed centrifugation steps. After addition of SDS-Laemmli sample buffer and heating at 50 °C for 30 min the equivalent of ~1–2 oocytes per lane was loaded on 10% SDS polyacrylamide gels [23], separated by electrophoresis, and transferred to PVDF membranes. Immunodetection was carried out using rabbit polyclonal antibody anti-ABD directed against the central hydrophilic domain (Lys1005 to Lys1321) of ATP7B [24] or, in case of HA-epitope-tagged constructs, using rat monoclonal anti-HA antibody 3F10 (Roche Molecular Biochemicals, Mannheim, Germany) and secondary AP- or HRP-conjugated goat anti-rabbit/anti-rat IgG (Jackson Immuno Research, Soham, U.K.) antibodies, respectively. Reacting proteins were visualized using the AP color reagent (Bio-Rad, Hercules, CA), or using the LumiLight western blotting substrate (Roche Molecular Biosciences, Mannheim, Germany) and detection on a Kodak BioMax film.

2.4. The ATP7B constructs for expression in Sf9 cells

Generation of recombinant baculoviruses and expression of wild-type ATP7B and its Asp1027Ala mutant were performed as described previously (33). To express the ATP7B-HA56 construct in *Sf9* cells, the ATP7B-pTNPN-HA56 plasmid was cut with Bsu36I enzyme to excise the region coding for ATP7B-HA56. The resulting fragment was cloned into the pFastBacDual-ATP7B plasmid (33), and digested with the same restriction enzyme. The resultant plasmid pFastBacDual-ATP7B-HA56 (pATP7B) was then utilized to generate the recombinant ATP7B-expressing baculovirus using previously described protocols [25] and the commercially available Bac-to-Bac kit (Invitrogen). DH10 Bac cells were transformed with pFastBacDual-ATP7B-HA56 and allowed to generate bacmids via the transposition mechanism as previously described [26]. The ATP7B bacmids were then used to transfect *Sf9* cells and produce baculovirus expressing ATP7B. Baculovirus was amplified as described in the Bac-to-Bac™ manual and in [25].

Table 1
Constructs used in this study

ATP7B HA-NT	HA-tag inserted after the initiating ATG codon
ATP7B HA 1,2	HA-tag inserted after Val683
ATP7B HA 3,4	HA-tag inserted after Ala756
ATP7B HA 4,5	HA-tag inserted after Ser797
ATP7B HA 5,6	HA-tag inserted after Asn958
ATP7B HA 7,8	HA-tag inserted after Ile1346
ATP7B HA-CT	HA-tag inserted before the Stop codon
ATP7B HA5,6 D1027A	ATP7B HA5,6 Asp1027Ala
ATP7B HA5,6 H1069Q	ATP7B HA5,6 His1069Gln
ATP7B HA5,6 del N600	Deletion of sequence Pro2–Ala600
ATP7B HA 5,6 del LLL	C-terminal deletion after Ser1453
ATP7B HA5,6 TGE>AAA	Replacement of the T585GE587 motive with AAA
ATP7B HA 5,6 CPC>SPS	Replacement of the C1014PC1016 with SPS

2.5. ATP7B Expression in insect cells and preparation of membrane fractions

Sf9 cells (Invitrogen) were maintained at 27 °C in 150 ml suspension cultures in Ex-Cell™ 420 growth medium (JRH Biosciences Inc., Lenexa, KS) and were split every 2–3 days with fresh medium to maintain cell densities between 0.5×10^6 and 4×10^6 cells/ml. Cells were infected with recombinant virus as previously described [25,27] and harvested 3 days post-infection. To obtain a total membrane preparation, the cells were centrifuged at 500 ×g for 10 min and the cell pellet was frozen at −20 °C and then thawed to facilitate lysis. Cells from a 50 ml culture were pelleted and resuspended in 4 ml of homogenizing buffer (HB): 25 mM imidazole, pH 7.4, 0.25 M sucrose, 1 mM dithiothreitol (1 tablet of Roche complete® protease inhibitor mixture was added per 50 ml of buffer solution). Cells were then lysed by a 20-stroke homogenization in a Dounce homogenizer, and centrifuged for 10 min at 500 ×g. The pellet was discarded and the soluble fraction was subjected to an additional centrifugation for 30 min at 20,000 ×g to sediment cell membranes. The membranes were then resuspended in 0.5 ml of HB and stored frozen at −80 °C until further use.

2.6. Phosphorylation of ATP7B from [γ^{32}P]-ATP

50 μg of total membrane protein was resuspended in 200 μl of the assay buffer: 20 mM bis-Tris propane, pH 6.0, 200 mM KCl, 5 mM $MgCl_2$. Radioactive [γ^{32}P]-ATP (5 μCi, specific activity 20 mCi/μmol) was added to a final concentration of 1 μM and the reaction mixture was incubated on ice for 4 min. The reaction was stopped by addition of 50 μl of ice-cold 1 mM NaH_2PO_4 in 50% trichloroacetic acid and then centrifuged for 10 min at 20,000 ×g. The protein pellet was washed once with ice-cold water and resuspended in 40 μl of sample buffer (5 mM Tris–PO_4, pH 5.8, 6.7 M urea, 0.4 M dithiothreitol, 5% SDS) and loaded on the acidic 7.5% polyacrylamide gel [28]. After electrophoresis, the gels were fixed in 10% acetic acid for 10 min and dried on blotting paper. The dried gels were exposed either overnight to the Molecular Imaging screen CS (Bio-Rad) or for several hours at −80 °C to the Kodak BioMax MS film and the intensity of the bands was quantified using a Bio-Rad Molecular Imager or Bio-Rad densitometer, respectively.

2.7. Post-embedding immunogold labeling, electron microscopy

X. laevis oocytes expressing different constructs of ATP7B were fixed at room temperature with 4% paraformaldehyde in combination with 0.1% or 0.5% or 1% glutaraldehyde either in PBS (in mM: 137 NaCl, 2.7 KCl, 7.4 Na_2HPO_4, 1.5 KH_2PO_4, pH 7.4) or in MBS (see above). After 3 h, the fixative was removed and oocytes washed with PBS and thereafter incubated overnight in 2% glycine/PBS. Cells were dehydrated in a series of increasing ethanol concentrations, infiltrated with LRWhite (London Resin Company Ltd, Reading, U.K.), transferred to gelatine capsules and polymerized at 55–60 °C. Thin sections were cut with the Ultracut microtome (Reichert, Vienna, Austria) and placed on Formvar® (poly vinyl formal) coated nickel grids (Plano GmbH, Wetzlar, Germany).

For immunogold labeling, thin sections were first incubated with saturated sodium metaperiodate (60 min), washed in water, treated sequentially with PBS + 2% glycine, PBS, PBS +1% BSA +0.1% Tween 20, PBS +0.1% BSA +0.05% Tween 20, and then reacted with the primary anti-ATP7B, anti-ABD antibody or, for the HA-tagged constructs, with the rat monoclonal anti-HA antibody 3F10 (Roche Molecular Biochemicals). Binding sites of the primary antibodies were visualized with secondary antibodies coupled to gold particles (diameters 10–12 nm, diluted 1:50 with PBS +0.1% BSA); goat anti-rabbit (Amersham Buchler, Braunschweig, Germany) or goat anti-rat (Aurion, Wageningen, The Netherlands), respectively. After washing off unbound secondary antibodies with PBS, sections were shortly treated with 1% glutardialdehyde in PBS, washed with water and dried. Before sections were analyzed in the electron microscope (EM208S, Philips, The Netherlands) they were contrasted with 2% uranyl acetate followed by 1% lead citrate.

2.8. Freeze-fracture replica labeling

For freeze-fracturing, unfixed oocytes were used. The oocytes were flattened and cut into four pieces with a razor blade. The yolk was washed away with Ringer solution and membrane pieces free of yolk were placed between two copper plates. These sandwiches were frozen in liquid nitrogen-cooled ethane. Fracturing and shadowing were carried out in a BAF T400 freeze-fracture machine (Balzers, Liechtenstein) with a pressure of $2 \cdot 10^{-7}$ b and by keeping the specimen stage at −140 °C. Platinum/carbon shadowing was performed using an angle of 45° and pure carbon evaporation was at an angle of 90°. Immunogold labeling of freeze-fracture replicas was performed according the protocol described in [29]. Briefly, replicas were thawed in 2.5% SDS in 10 mM Tris and 30 mM sucrose, pH 8.3, and after two changes of the SDS solution replicas were stirred overnight to dissolve organic material not in direct contact to the heavy metal replica sheet. Pieces of the replica were washed in PBS, then transferred to PBS +1% BSA and incubated for 2 h with the anti-ABD antibody (diluted 1:1000–1:2000 in PBS +0.1% BSA). To visualize the anti-ABD binding, samples were incubated with the secondary gold-ligated antibodies. After a washing step, the replicas were treated with 1% glutaraldehyde/PBS, washed with water and placed on Formvar® coated copper grids to be viewed in the electron microscope mentioned above. Images were taken with a CCD camera (TVIPS 1Kx1K slow-scan CCD camera, Tietz, Munich).

2.9. Surface detection of ATP7B in intact oocytes

Surface expression of the HA-tagged ATP7B constructs was measured as described in [30]. In short, oocytes were placed for 30 min in blocking solution BS (96 mM NaCl, 1 mM $MgCl_2$, 0.2 mM $CaCl_2$, 5 mM Hepes, 1% BSA, pH 7.4), incubated for 1 h with rat monoclonal anti-HA antibody 3F10 (Roche Molecular Biochemicals) diluted in BS (1 μg/ml), washed three times and incubated with HRP-conjugated secondary antibody (goat-anti-rat F_{AB} fragments; Jackson Immuno Research) in BS, followed by three washes each, first in BS, then in ND96 (96 mM NaCl, 1 mM $MgCl_2$, 0.2 mM $CaCl_2$, 5 mM HEPES, pH 7.4). All incubation and washing steps were carried out on ice. Surface expression was quantified by placing individual oocytes in 50 μl SuperSignal ELISA Femto Maximum Sensitivity Substrate solution (Pierce Biotech, Rockford, IL) and luminescence was measured in a TD 20/20 luminometer (Turner Designs, Sunnyvale, CA).

2.10. Data presentation and statistical analysis

Data analysis and presentation was carried out with Origin 7 software (OriginLab, Northampton, MA). Significance of normalized surface expression data was probed using *t*-test (Orgin 7).

3. Results

3.1. Expression of the full-length ATP7B in oocytes

To identify optimal conditions for protein expression, oocytes were injected with increasing amounts of ATP7B cRNA or water (control) and incubated for different periods of time; the membrane fractions were isolated, and the protein expression was analyzed by Western blot analysis. Immunostained bands corresponding to the 165 kDa protein were observed in the cRNA-injected oocytes, but not in the water-injected oocytes, indicating expression of the full-length ATP7B (Fig. 2A). The protein abundance increased according to the amount of injected RNA and it was maximal with 25 ng cRNA per oocyte. The expression levels did not increase with prolonged time (more than 4 days, data not shown). Therefore, injections with 25 ng cRNA were used as a standard for ATP7B expression and further analyses were carried out after 4 days post-injection.

3.2. Generation and characterization of the HA-tagged ATP7B for analysis of cell surface expression

To allow for surface detection of ATP7B, we inserted the YPYDVPDYA sequence (the HA-epitope) in each one of the

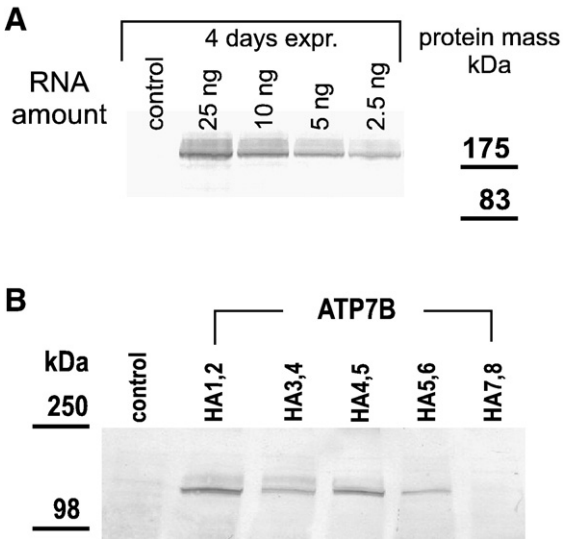

Fig. 2. Detection of ATP7B expression in *Xenopus* oocytes. (A) Different amounts of ATP7B wild-type cRNA were injected into oocytes, and cells were harvested after 4 days. Samples corresponding to the amount of one oocyte were loaded in each lane, and detection carried out with polyclonal antibody anti-ABD. (B) Comparison of protein expression for the ATP7B variants containing an HA-epitope inserted in the predicted extracellular loops. Control: Water-injected oocytes.

predicted extracellular loops (Fig. 1C): after Val683 (ATP7B-HA1,2), after Ala756 (ATP7B-HA3,4), after Asn958 (ATP7B-HA5,6), and after Ile1346 (ATP7B-HA7,8). For the extracellular loops between transmembrane segments (TMS) 3,4 and 7,8 two versions of inserts were generated: either with the standard HA-epitope, or with the HA-epitope plus an additional 6 amino-acid extension. The latter constructs were made to compensate for the fact that the extracellular loops between TMS3,4 and TMS7,8 of ATP7B are predicted to be very short, and the exposure and/or accessibility of the HA-epitope to the antibody could have been insufficient.

Expression of these constructs and subsequent Western blot analysis revealed that the ATP7B-HA1,2 and ATP7B-HA5,6 have similar expression (Fig. 2B), which was also similar or (for ATP7B-HA1,2) slightly higher than the non-tagged ATP7B (our data, not shown). In contrast, the protein expression was significantly reduced for ATP7B-HA3,4 when compared to ATP7B-HA1,2 or ATP7B-HA5,6. Hardly any protein was observed for ATP7B-HA7,8 variants with either the shorter or the longer insert (Fig. 2B). Consequently, only the ATP7B-HA1,2 and ATP7B-HA5,6 variants were used for further experiments.

Prior to evaluating the membrane targeting of ATP7B, the enzymatic activity of ATP7B-HA1,2 and ATP7B-HA5,6 was characterized to determine whether or not the epitope insertions had an effect on ATP7B function. The copper efflux experiments were hindered by the lack of sufficient copper uptake upon extracellular copper addition (our data, not shown) and by the complex cell response to injected copper. Consequently, to evaluate functionality of the tagged proteins we utilised a previously developed functional expression system in insect cells that produces high levels of heterologously expressed ATP7B. The ATP7B-HA1,2 and ATP7B-HA5,6 constructs were subcloned into the pFASTBacDual vector; corresponding baculoviruses were generated and the proteins were expressed in *Sf9* cells as described in [31].

The functional activity of HA-tagged ATP7B compared to the non-tagged control protein was evaluated by measuring formation of phosphorylated intermediate upon addition of ATP. The ATP7B mutant Asp1027Ala, in which the catalytic aspartate residue within the DKTG P-type ATPase signature motif (Fig. 1C) was exchanged for an alanine, served as a negative control. As in the oocyte system, in insect cells the HA-tagged ATP7B variants were expressed at comparable levels, but their functional activity was very different. The ATP7B-HA1,2 mutant had low levels of catalytic phosphorylation compared to either the wild-type or the ATP7B-HA5,6 protein (our data, not shown), suggesting that perturbation in the first extracellular loop alters either the efficiency of phosphorylation or the stability of the phosphorylated intermediate. In contrast, the levels of catalytic phosphorylation

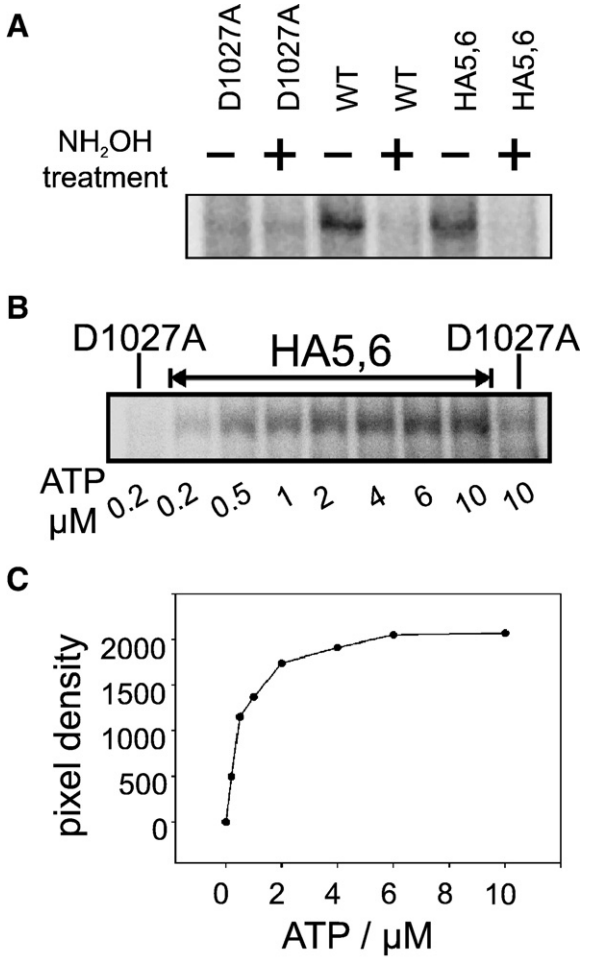

Fig. 3. Functional characterization of the epitope-tagged ATP7B-HA56 variant. ATP7B wild-type and ATP7B-HA56 proteins were expressed in *Sf9* cells and their functional properties were compared using phosphorylation assay with radioactive γ-ATP. (A) Control ATP7B and ATP7B-HA56 show comparable level of phosphorylation and similar sensitivity to treatments with hydroxylamine. No phosphorylation signal is visible for the catalytically inactive ATP7B-D1027A mutant (B) Dependence of phosphorylation level on the ATP concentration; mean values of two independent experiments are plotted (C) Densitometric evaluation of phosphorylation intensity yielded an apparent K_M for ATP of 0.5±0.15 μM.

for the ATP7B-HA5,6 construct were comparable to those of the wild-type ATP7B (Fig. 3A). Phosphorylation was sensitive to treatment with hydroxylamine, as was expected for the acyl-phosphate intermediate. No acyl-phosphate intermediate was detected for the inactive Asp1027Ala mutant. Finally, the analysis of the ATP-dependence of catalytic phosphorylation by ATP7B-HA5,6 yielded an apparent K_M of 0.5±0.15 μM for ATP (Fig. 3B, C). This value was comparable to the wild-type K_M for ATP (0.95±0.25 μM, [31]) confirming the proper folding and function of the ATP7B-HA5,6 variant. Consequently, the ATP7B-HA5,6 construct was used for targeting experiments and as a template for all other mutants described in this study.

3.3. The ATP7B-HA5,6 protein is targeted to the plasma membrane

Oocytes store large amounts of trace metals, which are fully sufficient for development of tadpole organs. Stage 6 oocytes were reported to contain 0.68±0.2 ng of copper corresponding to 0.01 mM in 1 μL eggs [32]. Our measurements of copper in oocytes using atomic absorption spectroscopy yielded higher values (about 50 μM), likely due to country-to-country variations in the metal content of drinking water in which the frogs are kept (data not shown). It is not known how much of this 50 μM copper is exchangeable and can be bound to ATP7B; consequently, we could not predict *a priori* whether ATP7B would be located in the intracellular compartments (as in low copper conditions in mammalian cells) or would traffic towards the plasma membrane (as would be expected when intracellular copper is elevated). To determine the intracellular localization of ATP7B-HA5,6, several experiments were carried out. First, immunogold labeling was performed on plastic sections of embedded oocytes expressing ATP7B-HA5,6. Two different antibodies (Abs) were used: the anti-HA Ab directed against the extracellular HA tag and anti-ABD, the antibody generated against the intracellular nucleotide-binding domain of ATP7B. Fig. 4 illustrates that in thin sections of permeabilized oocytes, both the anti-ABD (Fig. 4A) and anti-HA (Fig. 4B) antibody bind mostly to the oocyte microvillous cell membrane, indicating localization of ATP7B at the plasma membrane. In control oocytes injected with water, no gold marker was detected (Fig. 4C,D).

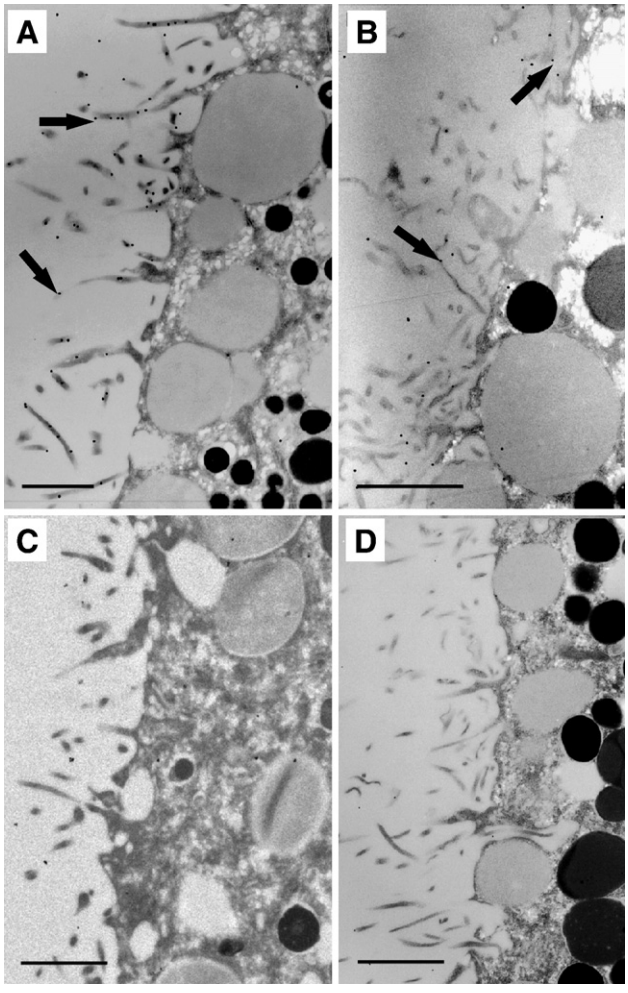

Fig. 4. Immunogold labelling of thin oocyte sections. Post-embedding immunogold labeling of oocyte sections was carried out with the polyclonal antibody anti-ABD (A,C), or the monoclonal anti-HA antibody 3F10 (B,D) of oocytes expressing either ATP7B wild-type (A) or ATP7B-HA(N) (B). Gold particles are present over microvilli of ATP7B-expressing oocytes (A,B) and not over uninjected controls (C,D). Representative areas of specific staining are indicated by black arrows. Scale bars=1 μm.

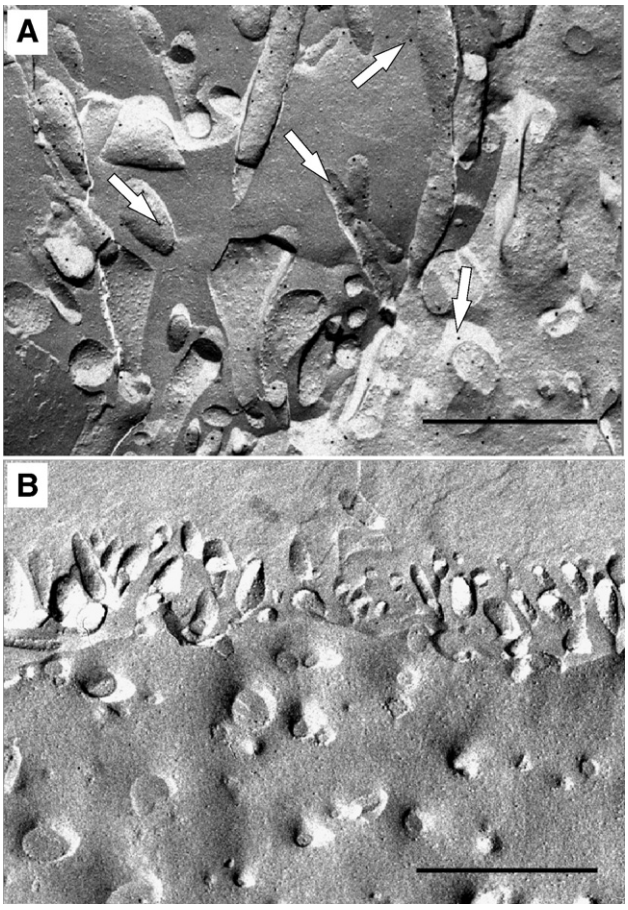

Fig. 5. Freeze-fracture replica labelling of *X. laevis* oocytes. Polyclonal antibody anti-ABD only binds to P(= plasmic)-fracture faces of ATP7B wild-type-expressing oocytes (A) and not to membranes of uninjected control oocytes (B). Representative areas of specific staining are indicated by black arrows. Scale bars=1 μm.

These results did not exclude the possibility that the expressed protein was localized to vesicles in immediate proximity to the plasma membrane and not at the membrane itself. Therefore, we utilized a freeze-fracture approach, which produces plasma membrane leaflets with characteristic appearances that allow verification of sidedness for membrane proteins or their domains. The immunostaining of freeze-fractured replicas of oocytes expressing ATP7B demonstrated the presence of the protein at the plasma membrane (Fig. 5A). Furthermore, the anti-ABD-coupled gold label was predominantly associated with the P(plasmic)-fracture face in agreement with the predicted cytoplasmic location of the nucleotide-binding domain of ATP7B (the antibody binding site). The replicas of control oocytes showed no labeling when treated with anti-ABD (Fig. 5B).

3.4. Utilization of HA-epitope tag allows quantitative analysis of ATP7B at the plasma membrane

For quantitative analysis of ATP7B at the plasma membrane, the presence of the HA tag at the cell surface was evaluated using the rat anti-HA antibody together with a goat-anti-rat horseradish peroxidase-coupled secondary antibody (HRP). The luminescence detection assay originally described by Zerangue et al. [30] for the plasma membrane localization of inward rectifier potassium channels was employed. Fig. 6A illustrates that the expression of ATP7B-HA5,6 in oocytes is associated with a luminescence signal, which has an amplitude more than fifty-fold higher than that in non-injected control oocytes. The injection of the non-tagged ATP7B showed no signal above background confirming the specificity of the assay.

To ensure that the oocytes were not leaky and only the extracellular HA-epitope was being detected, the HA tag was inserted at the N- and C-termini of ATP7B, which are predicted to be cytosolic. No surface luminescence was detected for the N-terminally-tagged construct despite the wild-type level of protein expression (our data, not shown). Similarly, the C-terminally tagged ATP7B showed no surface luminescence, but it was poorly expressed (or unstable) as indicated by low signal on a Western blot (our data, not shown). Finally, we tested whether or not ATP7B-HA5,6 is delivered to the plasma membrane if the amount of expressed protein is markedly decreased. The RNA titration experiments shown in Fig. 6B illustrate that surface luminescence is detected with as little as 2.5 ng of injected RNA. Under these conditions, both protein expression and surface targeting are well below saturation levels, arguing against the possibility that targeting to the plasma membrane is the result of protein overexpression.

To estimate how levels of ATP7B surface expression compare to that of a known plasma membrane protein, the HA-tagged bacteriorhodopsin was used. Bacteriorhodopsin is a type I transmembrane protein and the epitope was added to the extracellularly located amino-terminus (construct BR-NT-HA). The luminescence values for ATP7B-HA5,6 and BR-NT-HA were of equal magnitude within error limits (Fig. 6A), illustrating that the surface expression of ATP7B in oocytes is comparable to that of a typical plasma membrane protein.

3.5. The structural determinants participating in the trafficking of ATP7B are located outside of the N-terminal domain

The observed property of oocytes to robustly deliver ATP7B to the plasma membrane provided us with a very convenient system to identify factors important for trafficking of ATP7B. More than 80% of ATP7B residues are predicted to be in the cytosolic portion of the protein, including the large N-terminal domain with 6 copper-binding sites and the C-terminal tail, which contains the endocytic tri-leucine motif LLL (Fig. 1C). Previous studies in mammalian cells provided convincing evidence that the most of the N-terminal domain of ATP7B, including metal-binding sites 1–5, was not required for anterograde protein trafficking [33]. Deletion of the entire N-terminal domain of ATP7B, including the metal-binding sites 1–6, was also generated, however, the deleted protein was trapped in the endoplasmic reticulum, suggesting a problem with folding [33]. As a result, the role of the entire N-terminal domain could not be adequately evaluated. We reasoned that if the effect of the truncation on protein folding is not too great, it might be

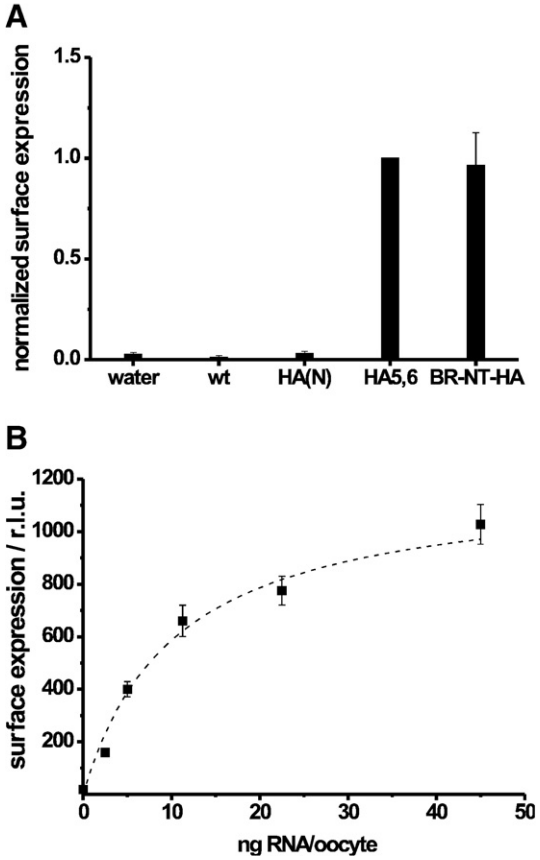

Fig. 6. Surface expression of ATP7B-HA5,6 (A) and cRNA dependence of surface expression (B). Within each experiment original luminescence data were averaged for each construct, normalized to the mean value for ATP7B-HA56 and then averaged for several experiments. Water-injected and ATP7B wild-type cRNA-injected oocytes served as background controls. Surface expression of an amino-terminally HA-tagged bacteriorhodopsin (BR-NT-HA) is shown for comparison. Experimental statistics (in brackets: number of batches/number of oocytes): water-injected. (20/191), WT (7/57), HA(N) (6,43), HA5,6 (25/256), BR-NT-HA (7/114). Data in (B) are averages of luminescence values for ATP7B-HA5,6 from one experiment with 15 to 20 oocytes per data point.

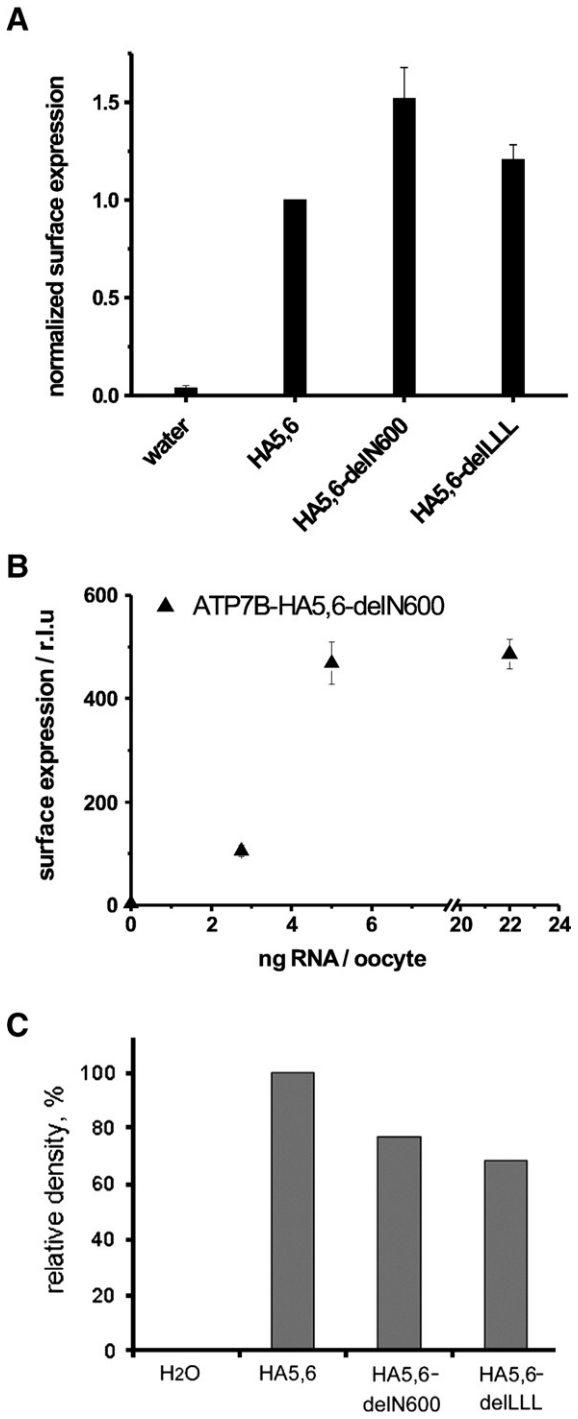

Fig. 7. The N-terminal and C-terminal deletions do not disrupt plasma membrane delivery of ATP7B-HA5,6. (A) Luminescence measurements of various ATP7B-HA5,6 constructs. Experimental statistics (in brackets: number of batches/number of cells): water-injected (15/178), HA5,6 (15/218), HA-5,6-delN600 (3/31), HA5,6-delLLL (3/38) (B) cRNA titration experiment to quantify the influence of the amount of cRNA injected on surface expression of ATP7B-HA5,6-delN600. Each data point corresponds to data from at least 10 cells. (C) Densitometry of a typical Western blot showing expression levels of the HA-5,6-delN600 and HA5,6-delLLL mutants of ATP7B compared to ATP7B-HA5,6 taken as 100%. Detection was carried out using anti-ABD antibody. Control: Water-injected oocytes (H_2O).

corrected in oocytes growing at 18 °C. Consequently, we generated the ATP7B-HA5,6-delN600 construct, in which the first 600 amino-acid residues were deleted, and characterized the expression and localization of this protein at the plasma membrane.

Fig. 7A illustrates that the expression of the ATP7B-HA5,6-delN600 mutant resulted in an excellent luminescence signal at the cell surface, which was 50% higher than that of the ATP7B-HA5,6 template construct. The cRNA molecules for the ATP7B-HA5,6-delN600 construct are significantly shorter than for ATP7B-HA5,6; consequently, a 25 ng injection sample for ATP7B-HA5,6-delN600 contains nearly 80% more cRNA molecules than one of ATP7B-HA5,6. To verify that the higher surface expression of ATP7B-HA5,6-delN600 was not due to a larger number of injected cRNA molecules, we carried out a cRNA titration experiment and measured surface expression of ATP7B-HA56-delN600 at lower cRNA levels. Fig. 7B illustrates that the surface expression of ATP7B-HA56-delN600 did not decline upon reduction of the injected cRNA, and it was decreased only when the amount of injected RNA was below 5 ng.

To ensure that the higher surface expression of ATP7B-HA5,6-delN600 variant is due to efficient delivery rather than much higher levels of protein expression, we compared total amounts of expressed ATP7B-HA5,6-delN600 and ATP7B-HA5,6 using densitometry of Western blots. Fig. 7C illustrates that ATP7B-HA5,6-delN600 was expressed on average at 45% of the level of ATP7B-HA5,6, yet it produced a higher level of surface expression. Thus, in oocytes, construct lacking the entire N-terminal domain traffics to the plasma membrane. In other words, the structural elements required for the delivery of ATP7B to the plasma membrane are located outside of the N-terminal domain. (It should be noted that the total amount of protein at the cell surface is determined by the rates of delivery and retrieval, and the proportionally higher surface expression of ATP7B-HA5,6-delN600 compared to ATP7B-HA5,6 could be due to changes in either step.)

Similarly, the truncation of ATP7B after Ser1453, in which the tri-leucine motif in the carboxy-terminus of ATP7B (the construct ATP7B-HA5,6-delLLL) was removed, decreased protein expression levels on average to approximately 67% of those of ATP7B-HA5,6 (Fig. 7C), but it was not detrimental to surface expression. In fact, the level of luminescence for ATP7B-HA5,6-delLLL was increased by 20%, consistent with the deletion of the putative endocytotic signal (Fig. 7A).

3.6. Catalytic activity is not required for ATP7B trafficking in oocytes

Current literature data do not provide a definitive answer as to whether or not the copper-ATPases have to be functionally active in order to traffic from the TGN. In order to resolve this question, at least for the oocyte system, we generated and characterized two mutants: the ATP7B-TGE>AAA, which mimics the phosphorylated state of the protein [20], and the catalytically incompetent Asp1027Ala, in which the catalytic phosphorylation was inactivated. The TGE>AAA mutant trafficked to the plasma membrane, although with slightly lower efficiency (Fig. 8A) compared to the control ATP7B-HA5,6 construct. The catalytically-incompetent mutant Asp1027Ala also showed wild-type level of luminescence at the plasma membrane, indicating that

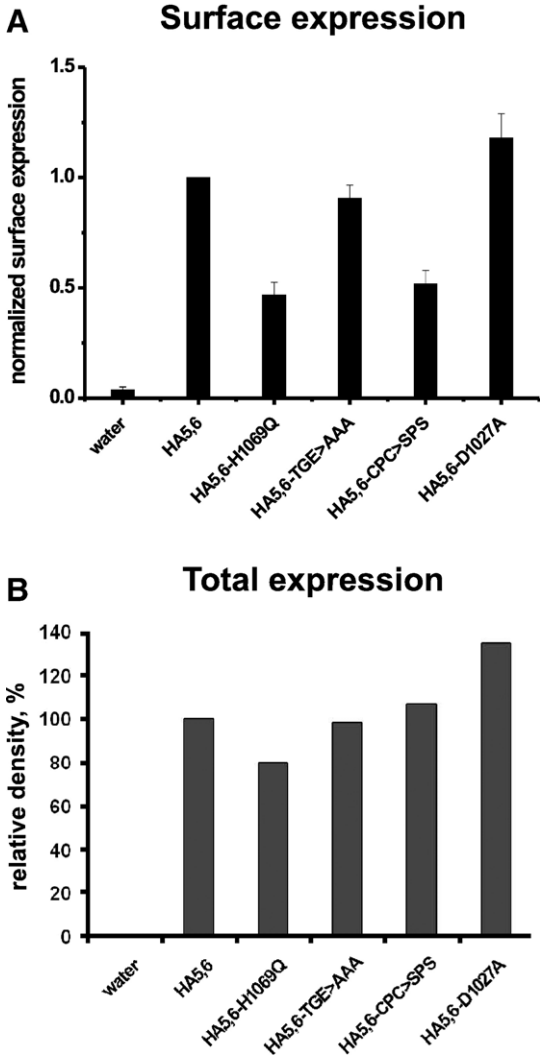

Fig. 8. The ability to bind ligands and not catalytic activity is required for plasma membrane delivery of ATP7B. (A) Luminescence measurements of various ATP7B-HA5,6 mutants. Experimental statistics (in brackets: number of batches/number of cells): water-injected (15/178), HA5,6 (15/218), HA5,6-H1069Q (3/69), HA5,6-TGE>AAA (6/112), HA5,6-CPC>SPS (6/113), HA5,6-D1027A (3/40). (B) Densitometry of a representative Western blot; expression of ATP7B-HA5,6 is taken as 100%. The detection was carried out using polyclonal antibody anti-ABD, the equivalent of 1.5 oocytes was loaded in each lane. Control: Water-injected oocytes.

activity and the ability to form a phosphorylated intermediate were not essential for the delivery of ATP7B to the plasma membrane (Fig. 8A). We hypothesized that it is not activity itself, but rather the ability of protein to bind ligands and/or achieve certain conformation(s) that modulate efficient delivery of ATP7B to the cell surface of oocyte.

To test this hypothesis, we generated and characterized two additional mutants. In the ATP7B-HA5,6-CPC>SPS mutant, the cysteine residues that coordinate copper in the membrane were substituted with serine residues. This mutation inactivates ATP7B [18] by markedly decreasing the ability of ATP7B to bind copper and undergo copper-induced conformational changes. In the ATP7B-HA5,6-H1069Q mutant, the invariant His1069 was replaced with Gln (a common Wilson disease mutation); this mutation markedly decreases the affinity of ATP7B for ATP [15,16]. In contrast to the Asp1027Ala mutant, which was targeted to the plasma membrane at the wild-type level (see above), both ATP7B-HA5,6-CPC>SPS and ATP7B-HA5,6-H1069Q produced significantly reduced luminescence (about 50%) at the cell surface (Fig. 8A). In the case of the ATP7B-HA5,6-H1069Q mutant, this decrease can be partially explained by a decrease in protein expression or stability, as the total levels of protein are, on average, at 65% of ATP7B-HA5,6 levels (Fig. 8B). By contrast, the ATP7B-HA5,6-CPC>SPS mutant is expressed at 107% of ATP7B-HA5,6 (Fig. 8B), yet it is significantly less abundant at the plasma membrane. These different trafficking characteristics of various mutants suggest that the ability to bind ligands/be stabilized in a certain conformation plays an important role in the ability of ATP7B to reach and/or be retained at the plasma membrane.

4. Discussion

In this work, we have developed a system for quantitative characterization of ATP7B at the plasma membrane. This was done by generating a functionally active ATP7B variant with an epitope-tag inserted into the extracellular loop and subsequent expression of this protein in *Xenopus* oocytes. The plasma membrane localization and sidedness for ATP7B have been established using electron microscopy and luminescence measurements. The system we have developed has significant advantages for studies in which access to both sides of ATP7B in the membrane is necessary, such as detailed analysis of protein topology, regulation of protein conformation by ligand binding, and studies of protein dynamics. None of these measurements can be easily done in mammalian cells. Our ability to directly quantify ATP7B at the cell surface also provides unique opportunity to examine factors that alter the presence of ATP7B at the plasma membrane.

In general, *Xenopus* oocytes mimic protein trafficking in mammalian cells and their trafficking machinery is sensitive to the same inhibitors of endocytosis and exocytosis [34]. However, in the case of ATP7B we observed some differences between mammalian and oocyte systems. In contrast to mammalian cells, in which protein exit from the TGN requires increased copper concentration, in oocytes additions of copper were not necessary to see trafficking towards the plasma membrane. Similar plasma membrane targeting in the absence of copper treatment was also reported for ATP7A [35]. This apparent loss of copper-dependency is most likely due to a large pool of exchangeable copper, as oocytes are known to be metal-rich. In mammalian cells, additions as low as 1 μM copper induce ATP7B trafficking [7]. Thus, it is conceivable that in oocytes, where the endogenous copper concentration in our experiments was 50 μM, there was a sufficient amount of exchangeable copper to induce constitutive trafficking of ATP7B. Our attempts to decrease intracellular copper concentration by injecting the copper chelator bathocuproine disulfonate were not tolerated by the oocytes; this has prevented us from directly testing the effect of copper on plasma membrane delivery of ATP7B in the oocyte system.

The presence of ATP7B at the plasma membrane may also reflect a shift in a steady-state distribution of the transporter due

to a much slower rate of endocytosis in oocytes compared to mammalian cells. Whatever the mechanism, it is clear that the efficiency of plasma membrane delivery or retention can be modulated by changes in the structure of ATP7B. Mutations that diminish the ability of ATP7B to bind important physiological ligands (ATP or especially Cu) decrease surface expression. In contrast, the deletion of the entire N-terminal domain is without significant effect. This last observation indicates that the delivery and retention at the plasma membrane do not require the N-terminal domain. Previous work using various modifications of the N-terminal domain of ATP7B revealed that the N-terminal domain contains sequence signal(s) within the first 63 N-terminal residues, which help to direct ATP7B towards the appropriate (apical) membrane in polarized hepatocytes [36]. Loss of these signals results in a copper-independent relocalization of ATP7B towards the basolateral membrane – a phenotype resembling ATP7B behaviour in the oocytes. Altogether, these results suggest that the sites of interaction with cell trafficking machinery are located outside of the ATP7B N-terminus, while the N-terminal region may modulate these interactions and/or provide extra contacts to ensure correct distribution of the transporter in polarized cells. Such a modulatory role mediated through protein–protein interactions may explain why mutations in the N-terminal domain of Cu-ATPases may prevent trafficking, while the deletion of the entire domain is permissive.

Our data also indicate that the catalytic activity or the formation of the phosphorylated intermediate are not essential for the plasma membrane delivery of ATP7B. The catalytically inactive Asp1027Ala mutant of ATP7B has not been characterized in mammalian cells, but several inactive mutants of homologous ATP7A were generated, and while many of them lost their ability to leave the TGN, other still could traffic [19–21]. These data and our present findings together suggest that stabilization of protein conformation rather than catalytic activity *per se* triggers protein trafficking. Biochemical characterization of mutants with different trafficking properties will help to elucidate which conformational state(s) of ATP7B are "trafficking-compatible".

Lastly, the developed system provides an excellent tool for determining the location of various ATP7B residues with respect to the membrane. ATP7B belongs to the 1B subgroup of P-type ATPases [5] and is predicted to have distinct membrane topology with 8 transmembrane segments (Fig. 1C). While such topology was confirmed for bacterial P_{1B}-ATPases (from *Helicobacter pylori* and *Escherichia coli*) [37,38], so far there have been no data on the topology of human copper-transporting ATPases. In this work, by inserting an epitope tag at various locations, we confirmed the intracellular localization of the N- and C-termini and the extracellular location of Val683 and Asn956 (the sites of HA1,2 and HA5,6 insertions, respectively). The introduction of the epitope into putative loops 3,4 and 7,8 led to misfolding and/or unstable products, as very little protein was detected. Thus, to better define the position of these loops a less invasive approach is necessary. The ability to target ATP7B to the plasma membrane and perform luminescence measurements has now opened the possibility to use less invasive techniques for topology analysis, such as Cys-scanning mutagenesis and surface biotinylation. It is also possible to study conformational changes at the protein surface in response to interactions with various ligands.

In summary, the studies of ATP7B in oocytes yielded direct evidence for plasma membrane targeting of ATP7B, illustrated the dependence of ATP7B trafficking on protein conformation rather than on activity, and supplied the first direct experimental evidence for ATP7B topology.

Acknowledgements

The authors thank Anja Becker, Verena Pintschovius, Eva Kaindl, and Friederike Joos for their excellent technical assistance, and Jan B. Koenderink and Jack H. Kaplan for the stimulating discussions. This work was supported by the Max-Planck-Society for the Advancement of Sciences and the Johann Wolfgang Goethe University of Frankfurt am Main and, in part, by the National Institute of Health grant RO1 DK071865 to S.L.

References

[1] S.A.K. Wilson, Progressive lenticular degeneration: a familial nervous disease associated with cirrhosis of the liver, Brain 34 (1912) 295–307.
[2] M.J. Czaja, F.R. Weiner, S.J. Schwarzenberg, I. Sternlieb, I.H. Scheinberg, D.H. Van Thiel, N.F. LaRusso, M.A. Giambrone, R. Kirschner, M.L. Koschinsky, et al., Molecular studies of ceruloplasmin deficiency in Wilson's disease, J. Clin. Invest. 80 (1987) 1200–1204.
[3] P.C. Bull, G.R. Thomas, J.M. Rommens, J.R. Forbes, D.W. Cox, The Wilson disease gene is a putative copper transporting P-type ATPase similar to the Menkes gene, Nat. Genet. 5 (1993) 327–337.
[4] R.E. Tanzi, K. Petrukhin, I. Chernov, J.L. Pellequer, W. Wasco, B. Ross, D.M. Romano, E. Parano, L. Pavone, L.M. Brzustowicz, et al., The Wilson disease gene is a copper transporting ATPase with homology to the Menkes disease gene, Nat. Genet. 5 (1993) 344–350.
[5] K.B. Axelsen, M.G. Palmgren, Evolution of substrate specificities in the P-type ATPase superfamily, J. Mol. Evol. 46 (1998) 84–101.
[6] M. Schaefer, R.G. Hopkins, M.L. Failla, J.D. Gitlin, Hepatocyte-specific localization and copper-dependent trafficking of the Wilson's disease protein in the liver, Am. J. Physiol. 276 (1999) G639–G646.
[7] H. Roelofsen, H. Wolters, M.J. Van Luyn, N. Miura, F. Kuipers, R.J. Vonk, Copper-induced apical trafficking of ATP7B in polarized hepatoma cells provides a mechanism for biliary copper excretion, Gastroenterology 119 (2000) 782–793.
[8] A.S. Payne, E.J. Kelly, J.D. Gitlin, Functional expression of the Wilson disease protein reveals mislocalization and impaired copper-dependent trafficking of the common H1069Q mutation, Proc. Natl. Acad. Sci. U. S. A 95 (1998) 10854–10859.
[9] Y. Guo, L. Nyasae, L.T. Braiterman, A.L. Hubbard, NH2-terminal signals in ATP7B Cu-ATPase mediate its Cu-dependent anterograde traffic in polarized hepatic cells, Am. J. Physiol.: Gastrointest. Liver Physiol. 289 (2005) G904–G916.
[10] A.T. Beggah, P. Beguin, K. Bamberg, G. Sachs, K. Geering, beta-subunit assembly is essential for the correct packing and the stable membrane insertion of the H,K-ATPase alpha-subunit, J. Biol. Chem. 274 (1999) 8217–8223.
[11] P. Beguin, A.T. Beggah, A.V. Chibalin, P. Burgener-Kairuz, F. Jaisser, P.M. Mathews, B.C. Rossier, S. Cotecchia, K. Geering, Phosphorylation of the Na,K-ATPase alpha-subunit by protein kinase A and C in vitro and in intact cells. Identification of a novel motif for PKC-mediated phosphorylation, J. Biol. Chem. 269 (1994) 24437–24445.
[12] P. Beguin, K. Geering, Structural domains implicated in ER degradation of alpha subunits of Na,K-ATPase, Ann. N. Y. Acad. Sci. 834 (1997) 540–542.

[13] D. Yoo, B.Y. Kim, C. Campo, L. Nance, A. King, D. Maouyo, P.A. Welling, Cell surface expression of the ROMK (Kir 1.1) channel is regulated by the aldosterone-induced kinase, SGK-1, and protein kinase, A. J. Biol. Chem. 278 (2003) 23066–23075.
[14] A.M. Sokac, C. Co, J. Taunton, W. Bement, Cdc42-dependent actin polymerization during compensatory endocytosis in *Xenopus* eggs, Nat. Cell Biol. 5 (2003) 727–732.
[15] R. Tsivkovskii, R.G. Efremov, S. Lutsenko, The role of the invariant His-1069 in folding and function of the Wilson's disease protein, the human copper-transporting ATPase ATP7B, J. Biol. Chem. 278 (2003) 13302–13308.
[16] O. Dmitriev, R. Tsivkovskii, F. Abildgaard, C.T. Morgan, J.L. Markley, S. Lutsenko, Solution structure of the N-domain of Wilson disease protein: distinct nucleotide-binding environment and effects of disease mutations, Proc. Natl. Acad. Sci. U. S. A 103 (2006) 5302–5307.
[17] M.L. Drumm, D.J. Wilkinson, L.S. Smit, R.T. Worrell, T.V. Strong, R.A. Frizzell, D.C. Dawson, F.S. Collins, Chloride conductance expressed by delta F508 and other mutant CFTRs in *Xenopus* oocytes, Science 254 (1991) 1797–1799.
[18] J.R. Forbes, D.W. Cox, Copper-dependent trafficking of Wilson disease mutant ATP7B proteins, Hum. Mol. Genet. 9 (2000) 1927–1935.
[19] J.F. Mercer, N. Barnes, J. Stevenson, D. Strausak, R.M. Llanos, Copper-induced trafficking of the cU-ATPases: a key mechanism for copper homeostasis, Biometals 16 (2003) 175–184.
[20] M.J. Petris, I. Voskoboinik, M. Cater, K. Smith, B.E. Kim, R.M. Llanos, D. Strausak, J. Camakaris, J.F. Mercer, Copper-regulated trafficking of the Menkes disease copper ATPase is associated with formation of a phosphorylated catalytic intermediate, J. Biol. Chem. 277 (2002) 46736–46742.
[21] I. Voskoboinik, J. Mar, J. Camakaris, Mutational analysis of the Menkes copper P-type ATPase (ATP7A), Biochem. Biophys. Res. Commun. 301 (2003) 488–494.
[22] C. Lorenz, M. Pusch, T.J. Jentsch, Heteromultimeric CLC chloride channels with novel properties, Proc. Natl. Acad. Sci. U. S. A 93 (1996) 13362–13366.
[23] U.K. Laemmli, Cleavage of structural proteins during the assembly of the head of bacteriophage, T4 Nature 227 (1970) 680–685.
[24] S. Lutsenko, M.J. Cooper, Localization of the Wilson's disease protein product to mitochondria, Proc. Natl. Acad. Sci. U. S. A 95 (1998) 6004–6009.
[25] Y.K. Hu, J.F. Eisses, J.H. Kaplan, Expression of an active Na,K-ATPase with an alpha-subunit lacking all twenty-three native cysteine residues, J. Biol. Chem. 275 (2000) 30734–30739.
[26] V.A. Luckow, S.C. Lee, G.F. Barry, P.O. Olins, Efficient generation of infectious recombinant baculoviruses by site-specific transposon-mediated insertion of foreign genes into a baculovirus genome propagated in *Escherichia coli*, J. Virol. 67 (1993) 4566–4579.
[27] C. Gatto, S.M. McLoud, J.H. Kaplan, Heterologous expression of Na(+)-K(+)-ATPase in insect cells: intracellular distribution of pump subunits, Am. J. Physiol. Cell Physiol. 281 (2001) C982–C992.
[28] B. Sarkadi, A. Enyedi, Z. Foldes-Papp, G. Gardos, Molecular characterization of the in situ red cell membrane calcium pump by limited proteolysis, J. Biol. Chem. 261 (1986) 9552–9557.
[29] K. Fujimoto, T. Noda, T. Fujimoto, A simple and reliable quick-freezing/freeze-fracturing procedure, Histochem. Cell Biol. 107 (1997) 81–84.
[30] N. Zerangue, B. Schwappach, Y.N. Jan, L.Y. Jan, A new ER trafficking signal regulates the subunit stoichiometry of plasma membrane K(ATP) channels, Neuron 22 (1999) 537–548.
[31] R. Tsivkovskii, J.F. Eisses, J.H. Kaplan, S. Lutsenko, Functional properties of the copper-transporting ATPase ATP7B (the Wilson's disease protein) expressed in insect cells, J. Biol. Chem. 277 (2002) 976–983.
[32] T. Nomizu, K.H. Falchuk, B.L. Vallee, Zinc, iron, and copper contents of *Xenopus laevis* oocytes and embryos, Mol. Reprod. Dev. 36 (1993) 419–423.
[33] M.A. Cater, J. Forbes, S. La Fontaine, D. Cox, J.F. Mercer, Intracellular trafficking of the human Wilson protein: the role of the six N-terminal metal-binding sites, Biochem. J. 380 (2004) 805–813.
[34] W.Z. Zeng, V. Babich, B. Ortega, R. Quigley, S.J. White, P.A. Welling, C.L. Huang, Evidence for endocytosis of ROMK potassium channel via clathrin-coated vesicles, Am. J. Physiol. Renal. Physiol. 283 (2002) F630–F639.
[35] K.D. Bissig, S. La Fontaine, J.F. Mercer, M. Solioz, Expression of the human Menkes ATPase in *Xenopus laevis* oocytes, Biol. Chem. 382 (2001) 711–714.
[36] Y. Guo, L. Nyasae, L.T. Braiterman, A.L. Hubbard, NH2-terminal signals in ATP7B Cu-ATPase mediate its Cu-dependent anterograde traffic in polarized hepatic. cells, Am. J. Physiol.: Gasterointest. Liver Physiol. 289 (2005) G904–G916.
[37] K. Melchers, T. Weitzenegger, A. Buhmann, W. Steinhilber, G. Sachs, K.P. Schafer, Cloning and membrane topology of a P type ATPase from *Helicobacter pylori*, J. Biol. Chem. 271 (1996) 446–457.
[38] K. Melchers, A. Schuhmacher, A. Buhmann, T. Weitzenegger, D. Belin, S. Grau, M. Ehrmann, Membrane topology of CadA homologous P-type ATPase of *Helicobacter pylori* as determined by expression of phoA fusions in *Escherichia coli* and the positive inside rule, Res. Microbiol. 150 (1999) 507–520.